19th Meeting of the Benelux EPR Society

Antwerp, 19th May 2011

Organizing Committee

Etienne Goovaerts

Sabine Van Doorslaer

19th Meeting of the Benelux EPR Society

19th May, 2011

Universiteit Antwerpen

Campus Middelheim, building G, room G.005

Programme

10.00 **Registration of participants. Coffee/Tea**

10.30 **Welcome**

10.35 *H. De Cooman (Universiteit Gent)*
Shallow intermolecular electron traps in organic crystals: an EPR/ENDOR/EIE study on sucrose

11.00 *M. Shabestari (Universiteit Leiden)*
Alzheimer amyloid peptide aggregation studied by SL-EPR

11.25 *M. Jivanescu (Katholieke Universiteit Leuven)*
Multi-frequency electron spin resonance analysis of the E'_δ defect in SiO_2 glasses

11.50 *Y. Ling (Universiteit Antwerpen)*
Light-induced EPR study of charge transfer in polymer/oligomer blends for organic photovoltaics

12.15 **Lunch**

13.45 *D.A.P. Nguyen (Katholieke Universiteit Leuven)*
Cr^+ contamination in near surface c-Si layers during ALD processing revealed by ESR

14.10 *M. Deschacht (Universiteit Antwerpen)*
Effects of Leishmania infection and treatment with antileishmanial drugs on the nitric oxide and superoxide response in macrophages

14.35 **Coffee/Tea Break**

15.00 *Q. Godechal (Université Catholique de Louvain)*
EPR spectrometry and imaging as a tool to study and characterize malignant melanoma

15.25 *P. Gast (Universiteit Leiden)*
Polarity effects on the g_x region of the EPR nitroxide powder spectra of spin labeled Sensory Rhodopsin

15.50 **General Assembly / Closing Remarks**

16.10 **Farewell drink**

Abstracts

B

Shallow intermolecular electron traps in organic crystals: an EPR/ENDOR/EIE study on sucrose

H. De Cooman[1,2,a], *A. Krivokapic*[3], *W.H. Nelson*[4], *M. Waroquier*[2] *and F. Callens*[1]

[1]*Department of Solid State Sciences, Ghent University, Krijgslaan 281-S1, 9000 Gent, Belgium*
[2]*Center for Molecular Modeling, Ghent University, Technologiepark 903, 9052 Zwijnaarde, Belgium*
[3]*Department of Physics, University of Oslo, P.O. Box 1048 Blindern, N-0316 Oslo, Norway*
[4]*Department of Physics and Astronomy, Georgia State University, Georgia 30303 (Atlanta), USA*
[a]*Postdoctoral Fellow of the Flemish Research Foundation (FWO-Vlaanderen)*

Exposure of organic matter to ionizing radiation mainly results in removal of electrons from molecular orbitals. These electrons therefore constitute the most primary product in reductive radiation damage. At room temperature, they recombine with cations or give rise to (excited) anionic molecules, which often are unstable and undergo subsequent chemical reactions. When irradiation is performed at sufficiently low temperature, however, expelled electrons can be trapped at intermolecular sites in an organic lattice, stabilized by the dipole moments of two or more neighboring OH-groups (*trapped electron*, TE). Annealing or UV radiation releases TEs from their traps, resulting in the same neutral molecular radicals that are formed when irradiation is performed at higher temperature. These TEs therefore allow studying the process of electron capture by an organic molecule and the subsequent radical formation. Such knowledge may among others assist in explaining radiation regioselectivity in biomolecules, *i.e.* the phenomenon of radiation inducing radicals preferentially at certain atoms.

In crystalline sucrose, the TE[1,2] as well as other radical species generated by X-ray irradiation at low temperature[3] have been well characterized using CW electron paramagnetic resonance (EPR), electron-nuclear double resonance (ENDOR) and ENDOR-induced EPR (EIE) measurements. Here, we present a detailed EPR/ENDOR/EIE study of the transformation of the TE into a molecular radical by annealing and UV illumination. The TE ap-pears to convert into a H-abstracted, C5-centered radical (R1, see figure) and a possible reaction mechanism, involving the generation of a H_2 molecule as a side product, is proposed.

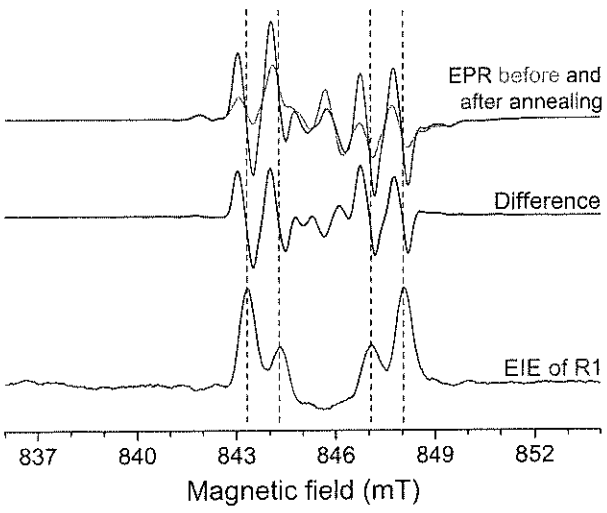

References

1. E.E. Budzinski, W.R. Potter, G. Potienko, H.C. Box, J. Chem. Phys., 70, 5040 (1979).
2. H.C. Box, E.E. Budzinski, H. G. Freund, J. Chem. Phys., 93, 55 (1990).
3. H. De Cooman, E. Pauwels, H. Vrielinck, E. Sagstuen, M. Waroquier, F. Callens, J. Phys. Chem. B, 114, 666 (2010).

Alzheimer amyloid peptide aggregation studied by SL-EPR

M.H. Shabestari[a], I. Sepkhanova[a], M. Drescher[a], N.J. Meeuwenoord[b], R.W.A.L. Limpens[c], R.I. Koning[c], D.V. Filippov[b], M. Huber[a]

[a]Department of Molecular Physics, Huygens Laboratory, Leiden University, P.O. Box 9504, 2300RA Leiden, The Netherlands
[b]Leiden Institue of Chemistry, Leiden University, Leiden, The Netherlands
[c]Leiden University Medical Center, Department of Molecular Cell Biology, Section Electron Microscopy, Leiden, The Netherlands

The aggregation of the β-Amyloid (Aβ) peptide into fibrils and plaques is the chief indicator of Alzheimer's disease. [1] Specific interest in oligomers stems from the suggestion that small, oligomeric aggregates and protofibrils, rather than fully formed fibrils could be responsible for the toxicity of the Aβ-peptide.

We investigate the potential of EPR to detect early stages of the aggregation of the Aβ-peptide. We have labeled the 40 residue Aβ peptide variant containing an N-terminal cystein (cys-Aβ) with the MTS spin label (SL- Aβ).

Continuous wave, 9 GHz EPR reveals three fractions of different spin-label mobility. One attributed to monomeric Aβ, one to a multimer (8 to 15 monomers), and the last one to larger aggregates or fibrils. (Fig. 1) The approach allows detection of oligomers on the timescale of aggregation. [2]

The future direction in this research is to study the effect of different conditions on the process of fibrilization and on the time scale of aggregation.

Fig. 1 simulation of the SL-Aβ spectrum with three components: dashed line fast, dotted line medium, short dashed line slow.

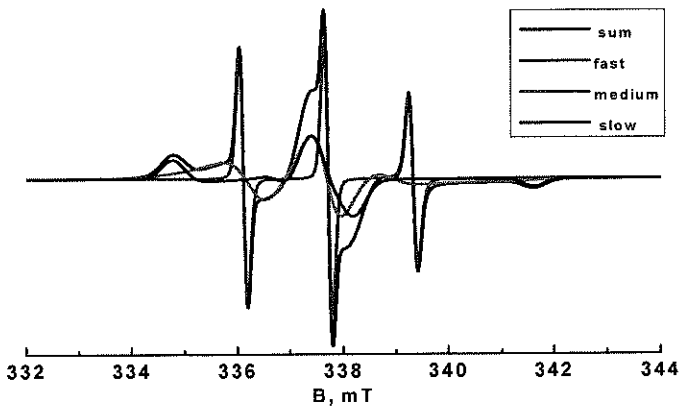

[1] Hardy, J. & Selkoe, DJ. Science, 297, 353-356. (2002)
[2] Sepkhanova, I., et al. Applied magnetic resonance, 36, 209-222. (2009)

HELAAS AFGELEGD

Multi-frequency electron spin resonance analysis of the E'$_\delta$ defect in SiO_2 glasses

Mihaela Jivanescu, A. Stesmans and V. V. Afanas'ev

Department of Physics, and INPAC –Institute for Nanoscale Physics and Chemistry, University of Leuven, Celestijnenlaan 200D, B-3001 Leuven, Belgium

X, K, and Q band electron spin resonance (ESR) study has been carried out on the nature of the E'$_\delta$ defect in amorphous (a-) SiO_2, both at cryogenic and room temperature, using two detection modes. In the attempt to activate E'$_\delta$ centers and increase their density, the six glasses investigated here have been subjected to various types of irradiation (UV, vacuum UV (VUV), and ^{60}Co γ-rays) and thermal treatment steps in air or Ar. To distinguish from the three atomic models (involving one unpaired electron delocalized over n = 2, 4 or 5 Si atoms) advanced in the literature for the E'$_\delta$ defect, the ESR intensity ratio (R_{hf}) of the 100-G ^{29}Si E'$_\delta$ hyperfine doublet to the corresponding central Zeeman signal is decisive. Reassuringly coinciding over all frequencies and measurement temperatures, the average R_{hf} value points to delocalization of the unpaired spin over n = 4 or 5 equivalent Si sites, thus refuting the theoretically propagated Si dimer (n = 2) model. The E'$_\delta$ signal could be generated only in three types of a-SiO_2, and only, yet always, by two types of irradiation, VUV and ^{60}Co γ-rays—not UV—suggesting that the E'$_\delta$ activation starts predominantly from preexisting sites through ionization processes. The invariance of the hf structure, both intensity and hf splitting, with measurement temperature points to an electronically rigid structure with no dynamic rearrangement occurring in the temperature range $T \geq 4.2$ K. An important finding is that E'$_\delta$ is only observed in those three silica types also showing the, possibly Na^+ compensated, Al E' center in the as γ-irradiated state. This may point to some indirect role of charge compensators/traps in activating/stabilizing E'$_\delta$ centers, relevant to further theoretical modeling.

Light-induced EPR study of charge transfer in polymer/oligomer blends for organic photovoltaics

Ling Yun[1], N. Nevil [1], S.Van Mierloo[2], D. Vanderzande[2], E. Goovaerts[1], S. Van Doorslaer[1]

[1] *Department of Physics, University of Antwerp, 2610 Antwerp, Belgium*
[2]*Institute for Materials Research (IMO), Hasselt University, B-3590 Diepenbeek Belgium*

Organic conjugated compounds are promising for the realization of low-cost, large-area electronic products like organic light-emitting diodes (OLED), field-emitting transitors (OFET) and organic solar cells. The 3D bulk heterojunction (BHJ) concept for solar cells starts from an intimate blend of donor ('p-type') and acceptor ('n-type') compounds. While a large number of p-type oligomers is now available, reports about n-type organic oligomer semiconductors are still scarce.

In this talk, we present a light-induced electron paramagnetic resonance (EPR) investigation of a series of potential n-type hexyl-substituted bisthiophene compounds (D1-D4) containing a thiazolothiazole(5,4-*d*) unit (scheme) [1] . Compounds D1-D4 were blended in different ratios with the standard p-type polymer MDMO-PPV (poly[2-methoxy-5-(3,7-dimethyloctyloxy)]-1,4-phenylenevinylene) to investigate possible electron transfer under illumination, an essential step in the photovoltaic process. X-band (9.44 GHz) CW EPR of these polymer/oligomer blends were measured before and after illumination with an Argon laser (λ=422 nm). This was compared with the results in the pure compounds D1-D4 and in MDMO-PPV and related to photoluminescence quenching experiments. The acceptor capacity as observed in the light-induced experiments in the blends is anti-correlated with the efficiency of iodine doping of the pure oligomers. The radical oligomer D4 resulting from iodine doping was fully characterized with pulsed EPR and DFT.

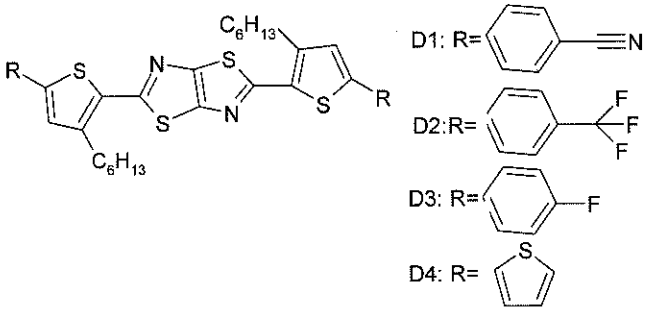

[1] S. Van Mierloo, et al. *Magn. Reson. Chem.***2010**, 48, 362-369

B

Cr^+ contamination in near surface c-Si layers during ALD processing revealed by ESR

Anh Phuc Duc Nguyen and Andre Stesmans.

Department of Physics and Astronomy,
University of Leuven,Celestijnenlaan 200D, 3001 Leuven

The atomic layer deposition (ALD) process is being widely used in nanotechnology for many reasons, one being its advantage as a low temperature process. The technique, however, may suffer from an inadvertent contamination, either in the deposited films or the substrate, potentially coming from precursors, catalysts, or reactor environment. Recently, a new process has been developed for deposition of high quality SiO_2 on Si, a self-catalytic reaction with novel properties [1]. High sensitivity low temperature electron spin resonance (ESR) analysis, however, has revealed unexpected contaminations. Using ESR, we observed a high local density of interstitial Cr impurities in near surface Si substrate layers, which could be reliably identified and quantified by detailed analysis of the ESR spectra, including field anisotropy, revealing the full crystal field effect details well known for interstitial Cr^+ in Si. Additionally, interstitial $(Fe_i)^0$ impurification has been detected as well, which together with the $(Cr_i)^+$ incorporation, refers to contamination resulting from the stainless steel reactor chamber walls or substrate holder.

[1] D. Hiller et al. J. Appl. Phys. 107, 064314 (2010)

Effects of *Leishmania* infection and treatment with antileishmanial drugs on the NO and $O_2^{\bullet-}$ response in macrophages

M. Deschacht, T. Van Assche, L. Maes and P. Cos.

Laboratory of Microbiology, Parasitology and Hygiene (LMPH), University of Antwerp, Groenenborgerlaan 171, B-2020 Antwerp, Belgium

Introduction: Despite the prominent role of reactive oxygen species (ROS) in the immune response against parasites, the intracellular protozoa *Leishmania* can survive in ROS-producing macrophages. This study investigated the effect of *Leishmania* infection and treatment with antileishmanial drugs on the oxidative response in macrophages.

Methods: Macrophages were infected with metacyclic promastigotes (10:1 parasite:macrophage ratio) and/or treated with pentavalent (Sb^{V}) and trivalent (Sb^{III}) antimony (256, 25.6 and 12.8 µg/ml), miltefosine (40 and 4 µM) or the experimental drug PX-6518 (10, 1 and 0.1 µg/ml). After 5 min, 2 h, 24 h and 48 h infection or treatment, cells were incubated with spin probe CM-H for measuring superoxide ($O_2^{\bullet-}$) or with spin trap $Fe(DETC)_2$ for measuring nitric oxide (NO) with EPR.

Results: At the beginning of the infection, $O_2^{\bullet-}$ levels increased significantly at 5 min (94.1 ± 13.8 % increase) and at 2 h (51 ± 9.9% increase), after which they fell back to basal levels. No pro-oxidant properties were observed after treatment. Moreover, dose- and time-dependent antioxidant properties were seen for Sb^{V}, Sb^{III}, PX-6518 and miltefosine.
NO production increased 24 h after infection with *L. infantum* 67 (45 ± 16.4 % increase) and *L. donovani* L82 (70 ± 27.1 % increase) metacyclic promastigotes. These data suggest an increase in NO production after *Leishmania* infection at a later time point compared to $O_2^{\bullet-}$ production. Drug treatment of uninfected cells did not affect significantly the NO response, although an increase for all of the drugs could be observed.
No significant increase in $O_2^{\bullet-}$ or NO in infected cells was observed after drug treatment.

Conclusion: Not only during the *Leishmania* infection itself but also during treatment with antileishmanial drugs ROS can play a crucial role. The use of the EPR technique in combination with a broad range of different *Leishmania* strains and drugs, makes that these results can be used to get more insight in the role of $O_2^{\bullet-}$ or NO during different infection stages.
$O_2^{\bullet-}$ seems to play an important role during phagosytosis of promastigotes, whereas amastigotes within the macrophage seem to influence the NO production.
Tested drugs had a (small) effect on NO and/or $O_2^{\bullet-}$ production in infected and/or treated macrophages, but none of these effects were significant or expected to be clinically relevant. These first data provide a good indication about the role of NO and $O_2^{\bullet-}$ in the activity of antileishmanial drugs. However, more experiments are necessary to obtain a correct and complete view on this subject.

3

EPR spectrometry and imaging as a tool to study and characterize malignant melanoma

Godechal Quentin, Levêque Philippe, Baurain Jean-François and Bernard Gallez.
Biomedical Magnetic Resonance Research Group. Louvain Drug Research Institute. Université catholique de Louvain.
Avenue Mounier 73, B-1200 Brussels Belgium

General introduction

Malignant melanoma is a skin tumor characterized by the uncontrolled proliferation of melanocytes, which can lead to metastasis mainly in lungs. The incidence of melanoma is rising each year. Nowadays, the cumulative lifetime risk for an invasive melanoma is estimated at 1/59 in U.S. For this reason, it is essential to develop new effective methods able to detect melanoma. The purpose of the present research was to assess the ability of EPR spectrometry and imaging to detect and characterize melanoma. In the first step of the work, the ability of EPR spectrometry to detect melanoma was compared with the bioluminescence (BLI) technique. The limit of sensitivity of the method was then assessed for X-Band (9GHz) and L-Band (1GHz). In the second step, EPR imaging was used to detect and characterize synthetic melanin-containing samples, *ex-vivo* B16 mouse melanomas and *ex-vivo* human melanomas.

First step: Assessment of melanoma extent and melanoma metastases invasion using EPR and bioluminescence imaging

Materials and methods

17 C57/BL6 mice were injected intravenously with 750.000 B16-luc cells. After 6, 15 and 18 days, mice were measured *in-vivo* with bioluminescence (Xenogen), the lungs were then excised, freeze-dried and measured by X-band EPR spectroscopy and imaging with a Bruker Elexsys spectrometer. Typical EPR parameters were: microwave power: 2.6 mW; modulation amplitude: 2.5G; sweep time: 30 seconds; number of scans: 10.

The same experiment was realized on 9 C57/BL6 mice injected with 750.000 B16-luc cells in the skin

The control experiment was realized in the same experimental conditions with 750.000 KHT-luc cells injected to C3H mice intravenously or subcutaneously.

Results

When EPR and BLI intensities were correlated with the weight of the samples, we observed that the correlation was clearly stronger for the EPR measurements than for BLI. This meant that EPR spectrometry seemed more suitable for the quantification measurements on melanoma. The experiments realized on non-pigmented KHT tumors demonstrated that the increase of EPR signal was linked to the presence of melanin and not only to the increase of tumor weight. The limit of detection of synthetic melanin by X-Band EPR was only 2 µg, but was 60 mg for melanoma powder measured in L-Band mode.

Second step: Towards an EPR image of human melanoma

Materials and Methods

3 synthetic phantoms, simulating the shape of *in-situ* skin melanomas, were created with melanin extracted from sepia officinalis. These melanoma-like samples were measured by EPR spectrometry and imaging with a Bruker Elexsys system working in X-Band mode (9GHz). Typical EPR parameters were: microwave power: 2.6 mW; modulation amplitude: 2.5 G; sweep time: 30 seconds; number of scans: 10.

3 mouse melanomas were obtained 8 days after injection of 750.000 B16 melanoma cells, freeze-dried or paraffin-embedded and measured in the same conditions than synthetic phantoms.

12 paraffin-embedded human skin melanoma samples (500 µm slice thickness; from the melanoma databank of Cliniques Universitaires Saint Luc) were measured and imaged using the same EPR system and parameters. 6 slices came from early growth stage melanoma (T1-T2) and 6 slices came from advanced melanoma (T3-T4).

Results

EPR imaging was able to detect and localize melanin pigments, both in synthetic phantoms and melanoma slices. The images obtained from synthetic samples were faithful to their respective models. The dimensions of these samples on the EPR images were very close to the real dimensions, with differences always below to 10% of the sample size. For mouse melanoma, well-delineated images could be obtained for samples thicker than 100µm, which seemed to be the limit of feasibility. The quality of human melanoma images was dependent on melanoma growth stage at the moment of excision. Advanced tumors (T3, T4) with high pigmentation provided relevant images, while early detected tumors (T1, T2) were generally too small to provide a sufficient signal for EPR imaging. The presence of EPR signals interfering with the signal of melanin was also observed on the spectra of T1 and T2 samples.

General discussion and conclusion

In a general way, we demonstrated that EPR spectrometry was an accurate tool to evaluate the extent of primary or metastatic melanomas. Moreover, EPR imaging was used for the first time to detect and localize melanin pigments inside human melanomas, without any contrast agent. However, and despite the good sensitivity of EPR X-Band spectrometry to detect melanin, it is for the moment difficult to get images from early stage (T1, T2) samples because of the poor signal-to-noise ratio in these samples, and the interferences with other EPR signals.

References: Godechal & al. Contrast Media and Molecular Imaging, in press. Godechal & al. Experimental Dermatology, submitted.

Polarity effects on the g_x region of the EPR nitroxide powder spectra of spin labeled Sensory Rhodopsin.

P. Gast[a], D. Stellinga[a], R. Herbonnet[a], L. Urban[b], J. Klare[b], H.J. Steinhoff[b], E.J.J. Groenen[a]

[a]Huygens Laboratory, Department of Molecular Physics, Leiden University, P.O. Box 9504, 2300 RA Leiden, The Netherlands, [b]Fachbereich Physik, Universität Osnabrück, Barbarastrasse 7, 49076 Osnabrück, Germany.

EPR studies of spin labeled proteins at 95 GHz have shown g_x regions in their nitroxide powder spectra that are more complex than was expected from X-band data [Bordignon *et al. Appl. Magn. Reson.* 2010, *37, 391-403*]. The single peak seen in this part of the spectrum at lower frequencies appears to split into three largely overlapping peaks. Measurements of the g values of these peaks have been compared with the polarity of the environment of the spin labels. The results seemed to be in agreement with the theoretical effects of hydrogen bond formation. However, the resolution at W-band is still low and the exact positions of the three peaks can not easily be determined. As a result the spread in the data is large enough to allow for significant error in the interpretation.

We measured the EPR powder spectra of a number of spin labeled proteins at 275.7 GHz. By comparing the hyperfine value A_{zz} with the g_x regions of the spectra we investigate the effects of local polarity on this part of the spectrum. We conclude that the three g values in the region are not dependent on polarity and that the three resolved peaks are related to the number of hydrogen bonds formed.

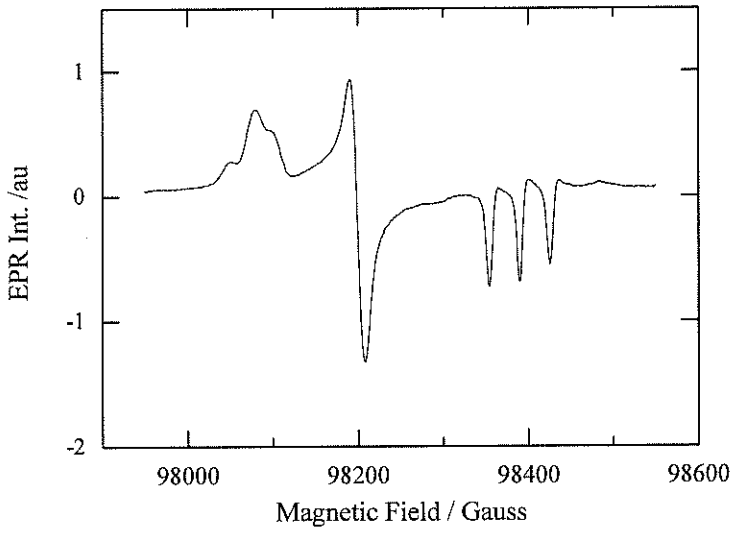

Typical example of a 275 GHz EPR spectrum of spin labeled Sensory Rhodopsin, measured using cw-detection at 40 K

Spin label changes

List of participants (registered on May 12, 2011) – Benelux EPR 2011

Blok	**Huib**	Universiteit Leiden	blok@physics.leidenuniv.nl.
Disselhorst	**Jos**	Universiteit Leiden	disselhorst@physics.leidenuniv.nl
Gast	**Peter**	Universiteit Leiden	gast@physics.leidenuniv.nl.
Groenen	**Edgar**	Universiteit Leiden	groenen@physics.leidenuniv.nl
Huber	**Martina**	Universiteit Leiden	huber@physics.leidenuniv.nl.
Kloek	**Jurriaan**	Universiteit Leiden	kloek@physics.leidenuniv.nl.
Mathies	**Jennifer**	Universiteit Leiden	mathies@physics.leidenuniv.nl.
Shabestari	**Maryam**	Universiteit Leiden	shabestari@physics.leidenuniv.nl
van Son	**Martin**	Universiteit Leiden	son@physics.leidenuniv.nl
Sottini	**Silvia**	Universiteit Leiden	sottini@physics.leidenuniv.nl.
Bernini	**Caterina**	Universiteit Leiden	bernini@physics.leidenuniv.nl
Yilmaz	**Duygu**	Rijksuniversiteit Groningen	duygu.yilmaz@rug.nl
Dimitrova	**Anna**	Rijksuniversiteit Groningen	a.i.dimitrova@rug.nl
Callens	**Freddy**	Universiteit Gent	freddy.callens@ugent.be
Vrielinck	**Henk**	Universiteit Gent	Henk.Vrielinck@UGent.be
Lauwaert	**Johan**	Universiteit Gent	Johan.Lauwaert@UGent.be
De Cooman	**Hendrik**	Universiteit Gent	hendrik.decooman@ugent.be
Pauwels	**Ewald**	Universiteit Gent	ewald.pauwels@ugent.be
Yavkin	**Boris**	Universiteit Antwerpen	Boris.Yavkin@ua.ac.be
Goovaerts	**Etienne**	Universiteit Antwerpen	Etienne.Goovaerts@ua.ac.be
Tedlla	**Biniam**	Universiteit Antwerpen	BiniamZerai.Tedlla@student.ua.ac.be
Van Doorslaer	**Sabine**	Universiteit Antwerpen	sabine.vandoorslaer@ua.ac.be
Feng	**Lin**	Universiteit Antwerpen	feng.lin@student.ua.ac.be
Ling	**Yun**	Universiteit Antwerpen	Yun.Ling@ua.ac.be
Deschacht	**Maartje**	Universiteit Antwerpen	maartje.deschacht@ua.ac.be
Godechal	**Quentin**	Université Catholique de Louvain	quentin.godechal@uclouvain.be
Marchand	**Valérie**	Université Catholique de Louvain	valerie.marchand@uclouvain.be
Leveque	**Philippe**	Université Catholique de Louvain	philippe.leveque@uclouvain.be
rao Singamaneni	**Srinivasa**	Université Catholique de Louvain	
Gallez	**Bernard**	Université Catholique de Louvain	bernard.gallez@uclouvain.be
Lobysheva	**Irina**	Université Catholique de Louvain	irina.lobysheva@uclouvain.be
Jivanescu	**Mihaela**	Katholieke Universiteit Leuven	mihaela.jivanescu@fys.kuleuven.be
Nguyen	**Duc A. P.**	Katholieke Universiteit Leuven	duc.nguyenahnphuc@fys.kuleuven.be
Kepa	**Jecek**	Katholieke Universiteit Leuven	
Penders	**Marc**	Bruker Belgium NV	Marc.Penders@bruker.be
van 't Hoff	**Ton**	Bruker Nederland BV	ton.vanthoff@bruker.nl